# Poly(Piloty's Acid): A Slow Releasing Macromolecular HNO Donor

Sarah N. Swilley, a Evan M. Zajkowskia, and John B. Matson\*a

<sup>a</sup>Department of Chemistry, Virginia Tech Center for Drug Discovery, Macromolecules Innovation Institute, 1040 Drillfield Dr., Blacksburg, VA 24061, USA.

**E-mail:** jbmatson@vt.edu

### **Abstract**

We report a polymeric version of Piloty's acid where the release rate of HNO can be tuned by changing the block ratios of PEG-b-poly(Piloty's acid) in a block copolymer system. The poly(Piloty's acid) block was derived from poly(styrene sulfonate), and HNO release from the block copolymers varied by as much as an order of magnitude via increasing the length of the poly(Piloty's acid) block. We anticipate this study will guide the development of HNO-releasing polymers to measure the effects of sustained HNO delivery in biological systems.

Nitroxyl (HNO, IUPAC name azanone) and nitric oxide (NO) are two endogenous signaling gases that differ in structure by a single hydrogen atom. They share some of the same biological activities such as vasodilation and cardioprotection, but they often operate through different mechanisms.<sup>1, 2</sup> For example, in the case of vasodilation, NO signaling operates using cGMP as a second messenger,<sup>3</sup> while HNO signaling is mediated by calcitonin gene-related peptide.<sup>4</sup> NO was identified as a biological signaling gas (often called a gasotransmitter) before HNO and has garnered more intensive study, but HNO has slowly gained attention as researchers have demonstrated its ability in animal models to inhibit tumor growth,<sup>5</sup> treat alcoholism,<sup>6</sup> and reduce the deleterious effects of heart failure,<sup>7</sup> among others. Piloty's acid (PA, Fig 1.) is a well-known HNO and NO donor that was first reported in 1896 and is quite stable in water at pH < 7.<sup>8</sup> At mildly basic pH, it can donate HNO, NO, or both together depending on the environment.<sup>9-11</sup>

Fig 1. Structure of Piloty's acid (PA).

The rate of dimerization of HNO (creating N<sub>2</sub>O after loss of water) is fast (8 x 10<sup>6</sup> M<sup>-1</sup>s<sup>-1</sup>), thus limiting the concentration of HNO in solution. 12, 13 Therefore, HNO gas cannot be delivered directly, so small molecule HNO donors such as PA have been used to probe the biological functions of HNO.<sup>4, 14-18</sup> Of the HNO donors, PA has been particularly well studied due to its chemical simplicity and long history. As such, many reports discuss various ways to tune HNO/NO release from small molecule PA derivatives, specifically by adding substituents to the ortho and/or para positions relative to the sulfonamide functional group. 19-22 In contrast, polymeric HNO donors have not been broadly studied, though polymeric systems for delivery of NO have been developed and investigated for decades with the goals of tuning release rates, enhancing bloodstream circulation time, and limiting toxicity.23 These same goals might be accomplished by polymeric HNO donors, specifically donors of PA, which could be useful in treating diseases and conditions that experience alkalosis (excessive alkalinity), <sup>24, 25</sup> where PA is most potent. In fact, only one report of a polymeric HNO donor has been published to our knowledge. In 2017, Boydston and coworkers developed an HNO delivery system via the slow thermal decomposition of an oxazine.<sup>26</sup> Inspired by this work, we asked whether the well-characterized HNO donor PA could be converted into a polymeric framework to control HNO release and provide a materials platform from which to deliver and study this important signaling molecule.

We set out to create a homopolymer of poly(Piloty's acid) (PPA) by performing a post-polymerization modification reaction on polystyrene sulfonate (PSS). The structural similarities between PA and PSS provided a potentially simple synthetic route to the target polymeric HNO donors. However, in initial trials we found that the limited solubility of PSS in organic solvents prevented clean conversion of PSS into PPA via a poly(sulfonyl chloride) intermediate. To circumvent this issue, we included a polyethylene glycol (PEG) component (5 kg/mol) to impart better solubility of the PEG-b-PSS block copolymers into thionyl chloride, which is necessary to convert the sulfonate groups into sulfonyl chloride groups (Scheme 1). We hypothesized that varying the PEG/PPA ratio by changing the molar mass of the PPA block in a block copolymer system would allow us to tune the rate of HNO release. Lastly, we set out to measure the pH dependence of HNO release from these macromolecular donors utilizing a turn-on fluorescent probe. We anticipated that as the pH of the environment and the amount of PA attached to the polymers increased, the rate of HNO release would also increase.

**Scheme 1** Synthesis of **PEG**<sub>110</sub>-*b***-<b>PPA**<sub>n</sub>. i. 4-vinylbenzenesulfonate (aka, sodium styrene sulfonate), H<sub>2</sub>O, 70 °C, 6 h; ii. ACVA, dioxane, reflux, 1 h; iii. SOCl<sub>2</sub>, reflux, 18 h; iv. NH<sub>2</sub>OH·HCl, MgO, H<sub>2</sub>O, MeOH, THF, rt, 18 h.

We performed RAFT polymerizations of 4-vinylbenzenesulfonate by using a previously reported macro chain transfer agent (CTA) with 5 kg/mol PEG on one end. 21 RAFT was carried out in water at 70 °C, followed by isolation of the polymer and treatment with azobis(4-cyanovaleric acid) (ACVA) to remove the dithioester end groups. Using this process, we generated a series of PEG<sub>110</sub>-b-PSS<sub>n</sub> block copolymers with degrees of polymerization (DPs) of 6, 15, 36, and 57 for the PSS blocks (Table 1). We estimated the DP of the PSS block of each block copolymer in three ways. First, we calculated an expected DP value by determining the % monomer conversion in the RAFT polymerizations via <sup>1</sup>H NMR spectroscopy. Second, we utilized <sup>1</sup>H NMR spectroscopy on the isolated block copolymers in D<sub>2</sub>O to determine block ratios by integrating the proton signals in the PEG backbone, known to correspond to DP = 110, and comparing these to the integrations of the proton signals in the PSS blocks (Figures S1-4†). Lastly, we estimated PSS block DPs using elemental analysis by comparing the carbon to sulfur ratios in each polymer (Figure S5, Tables S1-2†). In all four block copolymer samples, values generated by each of the three of these methods were close, suggesting that DP estimates were reasonably accurate. Aqueous size exclusion chromatography (SEC) was attempted but was not successful due to the tendency of the polymers to aggregate in solution.

**Table 1** Characterization of PEG-b-PSS block copolymers.

Block copolymer	· =	$M_{ m n,NMR}^b$	$M_{\rm n, EA}^c$
	kg/mol	kg/mol	kg/mol
PEG <sub>110</sub> -b-PSS <sub>6</sub>	6.8	6.4	6.4
PEG <sub>110</sub> -b-PSS <sub>15</sub>	9.5	8.6	8.0
PEG <sub>110</sub> -b-PSS <sub>36</sub>	12.6	10.2	12.0
PEG <sub>110</sub> -b-PSS <sub>57</sub>	16.7	17.1	15.8

<sup>a</sup>Expected  $M_n$  values based on % monomer conversion in the RAFT polymerization as measured by <sup>1</sup>H NMR spectroscopy. <sup>b</sup>Estimated  $M_n$  values determined by block analysis via <sup>1</sup>H NMR spectroscopy by comparing integral areas of the protons in the PEG backbone to those of the PSS backbone protons (D<sub>2</sub>O, Figures S1-4†). <sup>c</sup>Estimated  $M_n$  values based on elemental analysis where the degrees of polymerization were determined by C/S ratios (Table S2, Fig. S5†).

With a set of **PEG**<sub>110</sub>-**b**-**PSS**<sub>n</sub> block copolymers in hand, we then followed a reported twostep procedure to convert small molecule sulfonate groups into PA groups.<sup>22</sup> In brief, we first treated each of the **PEG**<sub>110</sub>-**b**-**PSS**<sub>n</sub> block copolymers with SOCl<sub>2</sub> to generate side chain sulfonyl chloride groups. Next, the sulfonyl chloride groups were converted into sulfonamides via the addition of hydroxylamine·HCl to give the final target block copolymer products, **PEG**<sub>110</sub>-**b**-**PPA**<sub>n</sub>. We confirmed the presence of sulfonamides by IR spectroscopy (Figure 2, Figures S6-8†) based on the peak shift from 1180 (sulfate) to 1160 cm<sup>-1</sup> (sulfonamide).

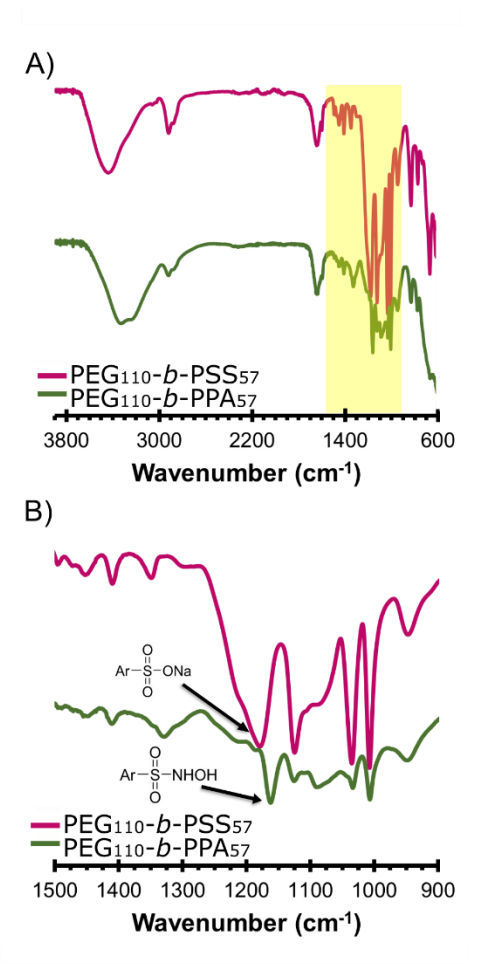


**Fig 2.** Representative FT-IR spectrum of sulfate to sulfonamide conversion in **PEG**<sub>110</sub>-*b*-**PSS**<sub>57</sub> to **PEG**<sub>110</sub>-*b*-**PPA**<sub>57</sub>. The top pink trace represents **PEG**<sub>110</sub>-*b*-**PSS**<sub>57</sub> while the bottom green trace represents **PEG**<sub>110</sub>-*b*-**PPA**<sub>57</sub>. (A) Full spectrum (B) Zoomed-in area highlighting the sulfate (1180 cm<sup>-1</sup>) and sulfonamide (1160 cm<sup>-1</sup>) peaks.

We characterized the series of four **PEG-b-PPA**<sub>n</sub> block copolymers using a variety of techniques to determine the degree of functionalization. SEC was attempted, but sample aggregation prevented accurate analysis. <sup>1</sup>H NMR spectroscopy was also not conclusive because the signals from the heteroatom protons were broad, and low signal from the quarternary carbon attached to the sulfonamide group prevented any definitive analysis by <sup>13</sup>C NMR spectroscopy. Instead, we again turned to elemental analysis to estimate the degree of functionalization of the block copolymer samples (Table 2, Table S3, Fig. S9†). By comparing C/N and S/N ratios of the **PEG**<sub>110</sub>-**b**-**PPA**<sub>n</sub> copolymers, we found that the degree of functionalization of the series of block copolymers ranged from 45–100% (Fig. S9, Table S3†).

Table 2 Characterization of PEG<sub>110</sub>-b-PPA<sub>n</sub> polymers.

<b>Block Copolymer</b>	% NHOH <sup>a</sup>	$Z_{\text{avg}}(\text{nm})^b$
PEG <sub>110</sub> -b-PPA <sub>6</sub>	100	$205 \pm 1$
PEG <sub>110</sub> -b-PPA <sub>15</sub>	89	$119 \pm 2$
PEG <sub>110</sub> -b-PPA <sub>36</sub>	45	$69 \pm 4$
PEG <sub>110</sub> -b-PPA <sub>57</sub>	74	19 ± 1

<sup>a</sup>Degree of functionalization determined by comparing both S/N and C/N ratios as calculated from elemental analysis (Table S3, Fig. S9†). <sup>b</sup>Z<sub>avg</sub> values as measured by dynamic light scattering (1 mg/mL, 20 mM pH 9 boric acid buffer, rt, Fig. S16†).

We examined the release rates of HNO from each of the four **PEG**<sub>110</sub>-*b*-**PPA**<sub>n</sub> block copolymers using the turn-on fluorescent HNO probe P-CM as reported from the Yu group.<sup>27</sup> Upon exposure to HNO, this probe releases 7-hydroxycoumarin (7-HC), accumulation of which can be monitored over time via fluorescence spectroscopy to determine the amount of HNO in solution. We used various buffers to follow release at different pH levels (either 20 mM PBS at pH 7.4 or 20 mM boric acid at pH 8, 9, or 10). These values were chosen in order to compare the HNO release profiles of the block copolymers to each other and to established literature values for the half-life of small molecule PA (36 h, 561 min, 90 min, and 33 min at pH 7.4, 8, 9, and 10, respectively<sup>9</sup>).

To carry out the release measurements, each block copolymer was dissolved in water at a concentration of 2 mM with respect to PA units, accounting for the degree of functionalization of each PPA block. Four solutions of the P-CM probe were prepared at pH 7.4, 8, 9, and 10 via dilution from a DMF stock solution. The probe and block copolymer solutions were then combined to reach a final concentration of 100  $\mu$ M probe and 200  $\mu$ M of PA units. HNO release was monitored via fluorescence spectroscopy over 12 h (n=3) at rt (Fig. 3A–C).

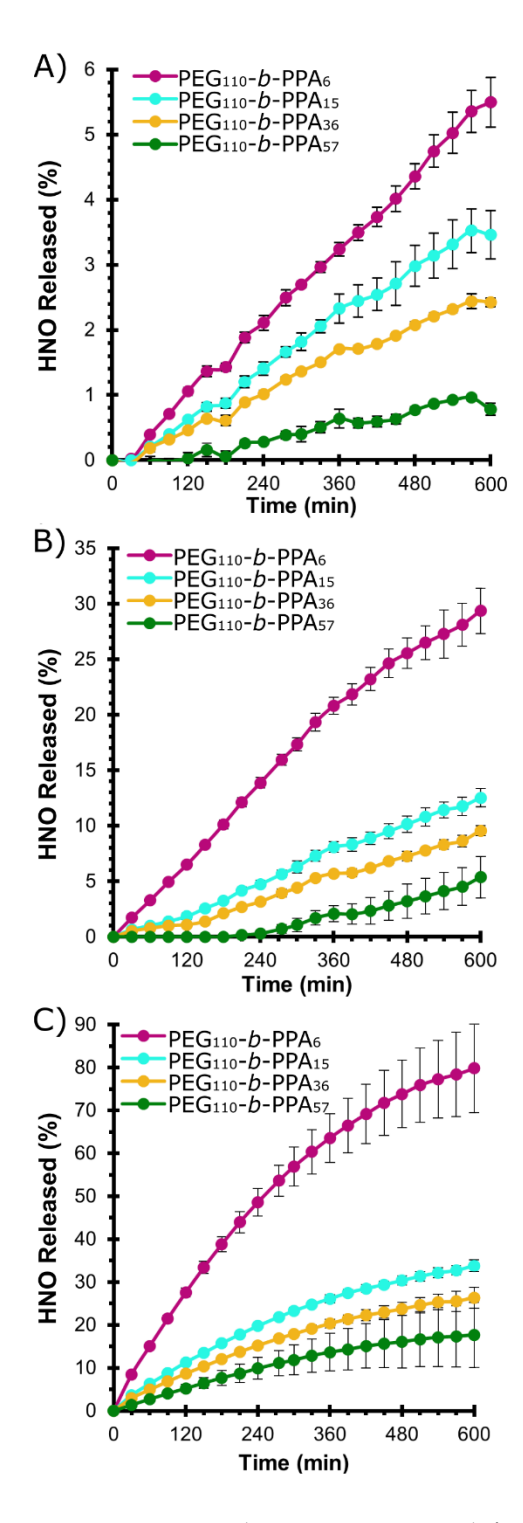


**Fig. 3** HNO release from **PEG**<sub>110</sub>-**b**-**PPA**<sub>n</sub> (n = 6, 15, 36, 57) in buffered aqueous solutions as measured over 10 h at rt. (A) 20 mM pH 7.4 PBS buffer. (B) 20 mM pH 8 boric acid buffer. (C) 20 mM pH 9 boric acid buffer.

To determine the maximum amount of HNO release for each block copolymer, we set the fluorescence intensity at 450 nm at pH 10 after 12 h to be 100% release, at which point the curves had plateaued (Fig. S10†). We then used these maximum values to normalize

the data for each of the four pH values to 100% release. Control studies with no probe confirmed our expectation that neither the PEG<sub>110</sub>-b-PPA<sub>n</sub> block copolymers nor their byproducts exhibited fluorescence themselves, validating that the observed increases in fluorescence were in fact due to released HNO from the block copolymers reacting with the P-CM probe (Fig. S11†). Furthermore, PEG<sub>110</sub>-b-PSS<sub>n</sub> block copolymers (without PA groups) were examined in the presence of P-CM (Fig. S12†), and the small amount of fluorescence observed was attributed to slow decomposition of P-CM in buffered solution on its own (Fig. S13†). To account for probe decomposition, we determined the HNO release profiles for all of the PEG-b-PPA<sub>n</sub> block copolymers by subtracting this background fluorescence from each curve (Fig. 3A–C).

A clear trend emerged upon analysis of these kinetic studies: As the DP of the PPA block increased, the HNO release rate decreased. For example, at pH 8 (Fig. 3B) **PEG**<sub>110</sub>-**b**-**PPA**<sub>6</sub> released 30% of its total HNO load over 10 h, while **PEG**<sub>110</sub>-**b**-**PPA**<sub>57</sub> released only 5%, with the **PEG**<sub>110</sub>-**b**-**PPA**<sub>15</sub> and **PEG**<sub>110</sub>-**b**-**PPA**<sub>36</sub> block copolymers releasing intermediate amounts. Additionally, as expected based on small molecule PA release rates, increasing buffer solution pH led to higher rates of HNO release (Fig. 4). For example, block copolymer **PEG**<sub>110</sub>-**b**-**PPA**<sub>6</sub> released just 6% of its total HNO load over 10 h at pH 7.4, and at pH 10 this value increased to 98%.

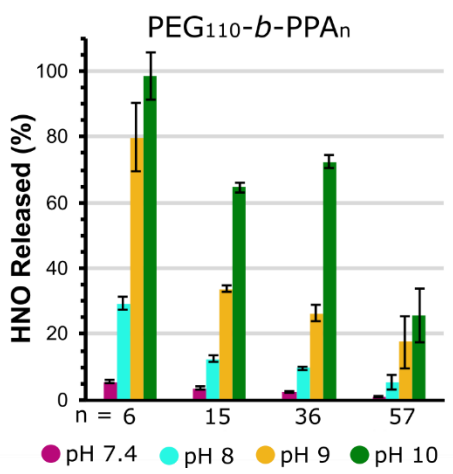


**Fig. 4** Bar graph summarizing HNO release results for the four PEG<sub>110</sub>-b-PPA<sub>n</sub> block copolymers at various pH values. Statistical analysis for the above figure can be found in Fig. S16†.

In order to explain the trends observed in the HNO release profiles, specifically the decreasing release rate as DP increased, we utilized dynamic light scattering (DLS) to measure the size of the block copolymer aggregates in solution. We found that PEG<sub>110</sub>-b-PPA<sub>6</sub> had a  $Z_{\rm avg}$  diameter of  $205 \pm 1$  nm and as the PPA chain length increased to PEG<sub>110</sub>-b-PPA<sub>57</sub> the  $Z_{\rm avg}$  decreased to  $19 \pm 1$  nm (Table 2, Fig. S18†). These results show that as the PPA block of the copolymers increased, the  $Z_{\rm avg}$  size of the particles decreased. This trend was unexpected because larger block copolymers tend to form larger aggregates. The smaller diameter in the polymer aggregates with longer PPA blocks must result from a decrease in aggregation number ( $N_{\rm agg}$ ). We speculate that the decreasing  $N_{\rm agg}$  values result from an increase in available sites for hydrogen bonding due to the introduction of the

nitrogen atom. This scenario is supported by several previously reported observations. First, in 2010 Hedrick and coworkers reported on a PEG copolymer system in which they examined the effects of incorporating different ratios of urea containing monomers with methylcarboxytrimethylene carbonate monomers. Their results showed that as the DP of the urea-containing block increased, these additional hydrogen bonding sites decreased the  $N_{\text{agg}}$  value of micelles in solution. Additionally, Whitmere and coworkers showed in 1989 that intermolecular interactions between PA small molecules gave rise to unusual molecular packing arrangements, for example where PA can pack into 16 membered hydrogen bonded rings. These previous observations support our suggestion that extensive hydrogen bonding exists in block copolymers with large PPA segments.

### **Conclusions**

In summary, we demonstrated a route to create a polymeric version of Piloty's acid, a well-known HNO donor. The sulfonate groups on PSS could be converted into PA groups, providing a straightforward method for making an HNO donor from the widely used polymer PSS. Utilizing a series of four block copolymers of the general structure PEG<sub>110</sub>-b-PPA<sub>n</sub>, we found that increasing the size of the PPA block in the copolymer extended the HNO release profile. At pH 7.4, PEG<sub>110</sub>-b-PPA<sub>6</sub> released 5.5% of its HNO load after 10 h, while PEG<sub>110</sub>-b-PPA<sub>57</sub> released less than 1%, indicating the ability to tune HNO release by changing the size of the polymer blocks. Because PA can donate NO as well as HNO, it is possible that these polymers could also be used as extended-release NO donors. We believe that this simple system may enable development of HNO releasing polymers to further study the effects of extended exogenous HNO release in biological systems.

### **Conflicts of interest**

There are no conflicts to declare.

## Acknowledgements

This work was supported by the National Science Foundation Division of Chemistry (CHE-2003662). This work was performed in part at the Nanoscale Characterization and Fabrication Laboratory, which is supported by the Virginia Tech National Center for Earth and Environmental Nanotechnology Infrastructure (NanoEarth), a member of the National Nanotechnology Coordinated Infrastructure (NNCI), supported by NSF (ECCS 1542100 and ECSS 2025151). We thank Prof. Andrew Lowell for use of the BioTek Cytation3 imaging reader and Dr. Jennifer McCord for her help with this instrument. We also thank Dr. Ryan Carrazzone and Dr. Kearsley Dillon for helpful suggestions.

#### **Notes and references**

- 1. J. C. Irvine, R. H. Ritchie, J. L. Favaloro, K. L. Andrews, R. E. Widdop and B. K. Kemp-Harper, *Trends Pharmacol. Sci.*, 2008, **29**, 601-608.
- 2. W. Flores-Santana, D. J. Salmon, S. Donzelli, C. H. Switzer, D. Basudhar, L. Ridnour, R. Cheng, S. A. Glynn, N. Paolocci, J. M. Fukuto, K. M. Miranda and D. A. Wink, *Antioxid. Redox Signal.*, 2011, **14**, 1659-1674.

- 3. W. P. Arnold, C. K. Mittal, S. Katsuki and F. Murad, *Proc. Natl. Acad. Sci.*, 1977, 74, 3203-3207.
- 4. N. Paolocci, W. F. Saavedra, K. M. Miranda, C. Martignani, T. Isoda, J. M. Hare, M. G. Espey, J. M. Fukuto, M. Feelisch, D. A. Wink and D. A. Kass, *Proc. Natl. Acad. Sci.*, 2001, **98**, 10463-10468.
- 5. A. J. Norris, M. R. Sartippour, M. Lu, T. Park, J. Y. Rao, M. I. Jackson, J. M. Fukuto and M. N. Brooks, *Int. J. Cancer*, 2008, **122**, 1905-1910.
- 6. E. G. DeMaster, B. Redfern and H. T. Nagasawa, *Biochem. Pharmacol.*, 1998, 55, 2007-2015.
- 7. N. Paolocci, G. Keceli, D. A. Wink and D. A. Kass, in *The Chemistry and Biology of Nitroxyl (HNO)*, eds. F. Doctorovich, P. J. Farmer and M. A. Marti, Elsevier, Boston, 2017, DOI: <a href="https://doi.org/10.1016/B978-0-12-800934-5.00019-0">https://doi.org/10.1016/B978-0-12-800934-5.00019-0</a>, pp. 353-387.
- 8. O. Piloty, Ber. Dtsch. Chem. Ges., 1896, 29, 1559-1567.
- 9. J. F. DuMond and S. B. King, *Antioxid. Redox Signal.*, 2011, **14**, 1637-1648.
- 10. H. Nakagawa, J. Inorg. Biochem., 2013, 118, 187-190.
- 11. R. Zamora, A. Grzesiok, H. Weber and M. Feelisch, *Biochem. J.*, 1995, **312**, 333-339.
- 12. V. Shafirovich and S. V. Lymar, *Proc. Natl. Acad. Sci.*, 2002, **99**, 7340-7345.
- 13. C. Fehling and G. Friedrichs, *J. Am. Chem. Soc.*, 2011, **133**, 17912-17922.
- 14. G. Keceli, C. D. Moore and J. P. Toscano, *Bioorg Med. Chem. Lett.*, 2014, **24**, 3710-3713.
- 15. G. Keceli and J. P. Toscano, *Biochemistry*, 2014, **53**, 3689-3698.
- 16. R. Y. Cheng, D. Basudhar, L. A. Ridnour, J. L. Heinecke, A. H. Kesarwala, S. Glynn, C. H. Switzer, S. Ambs, K. M. Miranda and D. A. Wink, *Nitric Oxide*, 2014, 43, 17-28.
- 17. T. W. Miller, M. M. Cherney, A. J. Lee, N. E. Francoleon, P. J. Farmer, S. B. King, A. J. Hobbs, K. M. Miranda, J. N. Burstyn and J. M. Fukuto, *J. Biol. Chem.*, 2009, **284**, 21788-21796.
- 18. D. Basudhar, G. Bharadwaj, R. Y. Cheng, S. Jain, S. Shi, J. L. Heinecke, R. J. Holland, L. A. Ridnour, V. M. Caceres, R. C. Spadari-Bratfisch, N. Paolocci, C. A. Velázquez-Martínez, D. A. Wink and K. M. Miranda, *J. Med. Chem.*, 2013, **56**, 7804-7820.
- 19. D. Sanna, G. Rocchitta, M. Serra, M. Abbondio, P. A. Serra, R. Migheli, L. De Luca, E. Garribba and A. Porcheddu, *Pharmaceuticals (Basel)*, 2017, **10**, 74.
- 20. K. Aizawa, H. Nakagawa, K. Matsuo, K. Kawai, N. Ieda, T. Suzuki and N. Miyata, *Bioorganic Med. Chem. Lett.*, 2013, **23**, 2340-2343.
- 21. R. Smulik-Izydorczyk, M. Rostkowski, A. Gerbich, D. Jarmoc, J. Adamus, A. Leszczyńska, R. Michalski, A. Marcinek, K. Kramkowski and A. Sikora, *Arch. Biochem. Biophys.*, 2019, **661**, 132-144.
- 22. D. A. Guthrie, N. Y. Kim, M. A. Siegler, C. D. Moore and J. P. Toscano, *J. Am. Chem. Soc.*, 2012, **134**, 1962-1965.
- 23. D. A. Riccio and M. H. Schoenfisch, *Chem. Soc. Rev.*, 2012, **41**, 3731-3741.
- 24. A. B. Faridi and L. S. Weisberg, in *Critical Care Medicine (Third Edition)*, eds. J. E. Parrillo and R. P. Dellinger, Mosby, Philadelphia, 2008, DOI: <a href="https://doi.org/10.1016/B978-032304841-5.50060-1">https://doi.org/10.1016/B978-032304841-5.50060-1</a>, pp. 1203-1243.

- 25. D. Eckstein and H. E. Corey, in *Critical Care Nephrology (Third Edition)*, eds. C. Ronco, R. Bellomo, J. A. Kellum and Z. Ricci, Elsevier, Philadelphia, 2019, DOI: https://doi.org/10.1016/B978-0-323-44942-7.00069-8, pp. 409-411.e401.
- 26. D. C. Church, S. Nourian, C.-U. Lee, N. A. Yakelis, J. P. Toscano and A. J. Boydston, *ACS Macro Lett.*, 2017, **6**, 46-49.
- 27. G.-J. Mao, X.-B. Zhang, X.-L. Shi, H.-W. Liu, Y.-X. Wu, L.-Y. Zhou, W. Tan and R.-Q. Yu, *Chem. Commun.*, 2014, **50**, 5790-5792.
- 28. S. H. Kim, J. P. K. Tan, F. Nederberg, K. Fukushima, J. Colson, C. Yang, A. Nelson, Y.-Y. Yang and J. L. Hedrick, *Biomaterials*, 2010, **31**, 8063-8071.
- 29. J. N. Scholz, P. S. Engel, C. Glidewell and K. H. Whitmire, *Tetrahedron*, 1989, **45**, 7695-7708.